

Transition from Spatiotemporal Chaos to Ideal Straight Rolls in Rayleigh-Bénard Convection

Reha V. Cakmur*, David A. Egolf†, Brendan B. Plapp, and Eberhard Bodenschatz‡,
Laboratory of Atomic and Solid State Physics, Cornell University, Ithaca, NY 14853-2501
 (February 9, 2008)

For Rayleigh-Bénard convection in a square cell with a fluid of Prandtl number one, we report experimental results on the transition between a stationary pattern of ideal straight rolls (ISR) and the spatiotemporal chaotic state of spiral defect chaos (SDC). In contrast to experiments in circular geometries, we found ISR states below a particular value of the control parameter and SDC states above this value. By characterizing the pattern with a global measure, the pattern entropy, we found that the transition from SDC to ISR showed similarities to phase transitions in equilibrium finite-size systems.

47.54.+r, 47.20.Lz, 47.27.Te

In recent years scientists in a number of fields have shown great interest in dissipative pattern-forming systems of large spatial extent. These systems often display particularly intriguing states of persistent time-dependent behavior termed spatiotemporal chaos [1–3]. One important question regarding these states is whether ideas from statistical mechanics may be useful for understanding the complex spatiotemporal behavior. In this Letter we present experimental data showing that a transition between a spatiotemporal chaotic state and a well-ordered time-independent state of Rayleigh-Bénard convection is similar to phase transitions in finite-size equilibrium systems [4].

In a Rayleigh-Bénard convection experiment, a horizontal fluid layer of height d is confined between a top plate of uniform temperature T_{top} and a bottom plate of uniform temperature $T_{\text{bottom}} = T_{\text{top}} + \Delta T$. For ΔT less than a critical value ΔT_c , the fluid is stationary; however, when $\Delta T > \Delta T_c$, the stationary state is unstable and a pattern of convection rolls with wavenumber $k \approx \pi/d$ develops [5]. For systems of infinite extent in the horizontal directions it was shown theoretically that an ideal pattern of straight rolls (ISR) of wavenumber k is stable in a restricted region of the $\epsilon - k$ parameter space [6], where $\epsilon = (\Delta T / \Delta T_c - 1)$ is the reduced control parameter. Experiments with argon gas in a rectangular cell of small aspect ratio $\Gamma = (\text{length}/2)/d \approx 15$ [7] showed reasonable agreement with these predictions. However, for a larger circular cell of radial aspect ratio $\Gamma = r/d = 76$, Morris *et al.* found a state of spatiotemporal chaos within the boundaries of the stable region of the $\epsilon - k$ parameter space [8]. This state, termed spiral defect chaos (SDC) and shown in Fig. 1(a), is characterized by a complex dynamics involving targets, rotating spirals, dislocations, disclinations, and grain boundaries. However, as shown in Fig. 1(a), SDC also shows narrow regions of slightly curved ISR. In this Letter we argue that it is the growth of these regions that characterizes the transition from

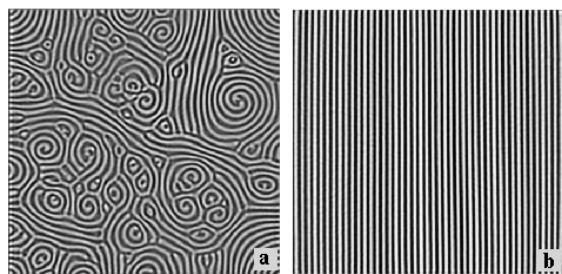


FIG. 1. (a) Spiral defect chaos and (b) ideal rolls at $\epsilon = 0.92$. Warm upflow corresponds to dark and cold downflow to bright.

SDC to ISR.

Since the discovery of SDC an unresolved question was whether the ISR predicted to be stable for an infinite system could be realized in a large aspect ratio experiment. Recently, Cakmur *et al.* used specially prepared systems and showed that ISR were indeed stable where predicted, and that both SDC states and ISR states existed for the same value of ϵ [9]. Fig. 1 shows two shadowgraph images illustrating this bistability.

Experiments in circular cells with fluids of small Prandtl number have suggested that above a particular value of ϵ , SDC is the state chosen for almost all initial conditions [10–12]. Just below this value of ϵ a time-dependent, apparently chaotic state without spirals was found. Earlier experimental and theoretical investigations of the latter state [1] led to the conclusion that the tendency of rolls to align perpendicularly to the boundaries necessarily results in roll curvature which, due to large-scale flows, leads to the observed persistent pattern dynamics. Motivated by these earlier observations, investigations of SDC were mostly limited to circular containers. Almost no experiments were conducted in rectangular cells [12], although pioneering experiments by Gollub and coworkers [13] had shown that ISR appeared after a

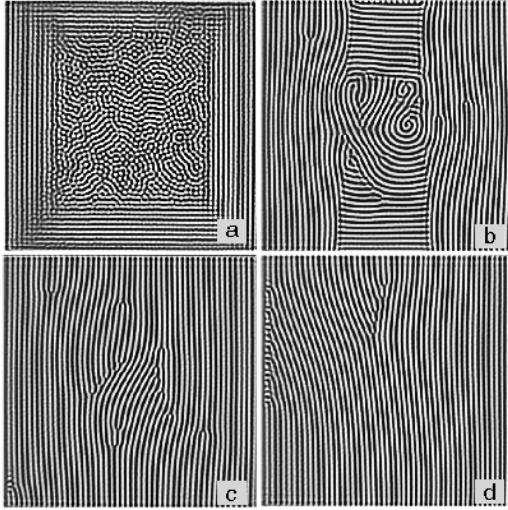


FIG. 2. Shadowgraph images of the convective pattern for a control parameter jump from below onset ($\epsilon < 0$) to above onset ($\epsilon = 0.233$) at times (a) $\sim 45\tau_T$, (b) $229\tau_T$, (c) $458\tau_T$, and (d) $22689\tau_T = 9.1\tau_h$, the stationary pattern.

long transient in a small aspect ratio rectangular cell. In the remainder of this Letter, we present quantitative experimental data from a large aspect ratio convection cell of square geometry showing that the transition between SDC and ISR exhibits similarities to equilibrium phase transitions in finite-size systems.

The experiment was conducted in a square cell with aspect ratio $\Gamma = (L/2)/d = 50$, where L is the length on a side. The fluid was CO_2 gas at a pressure of (41.593 ± 0.007) bar and Prandtl number $\sigma = \tau_T/\tau_\nu = 1.1$, where τ_ν is the vertical viscous timescale, $\tau_T = d^2/\kappa = 2.6$ s is the vertical thermal diffusion timescale, and κ is the thermal diffusivity [14]. The experimental setup was similar to that described in Ref. [10]. The cell's circular top and bottom sapphire plates were 1 cm thick, were spaced $(623 \pm 4) \mu\text{m}$ apart, and were parallel to within $\pm 3 \mu\text{m}$ over the 10 cm diameter. The top plate temperature was set at $(24.00 \pm 0.05)^\circ\text{C}$ by a circulating water bath and the bottom plate was heated by an electric film heater. Both temperatures were regulated to ± 0.3 mK, and the pressure was regulated to $\pm 5 \times 10^{-3}$ bar. For this experimental situation the parameters were sufficiently temperature independent so the Boussinesq approximation could be applied [14,15]. The bottom sapphire plate was coated with aluminum to allow the visualization of the pattern from above using the shadowgraph technique [10]. Eight circular paper sheets were placed between the top and bottom plates, and a square of size $100d$ was cut out of the center of the circular sheets to provide the boundary of the convection cell [16]. The measured onset of convection was (2.03 ± 0.02) K, which is in good agreement with the theoretical prediction of (2.04 ± 0.02) K.

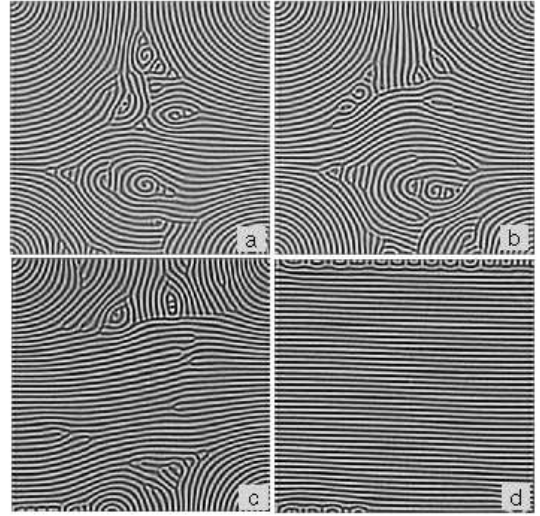


FIG. 3. Time evolution of the pattern for $\epsilon = 0.58$ at times (a) $13.70\tau_h$, (b) $13.80\tau_h$, (c) $14.07\tau_h$, and (d) $28.96\tau_h$, the stationary pattern.

For each value of the control parameter studied, the system was initialized by a jump from below onset ($\epsilon < 0$) to above onset ($\epsilon > 0$). After this jump, straight rolls initially formed near the sidewalls while a random pattern appeared in the middle of the cell. For $\epsilon \lesssim 0.53$, the pattern coarsened over time and developed after a transient into ISR with a few stray defects. An example of the pattern evolution is shown in Fig. 2. For $\epsilon \gtrsim 0.58$ the pattern did not order into ISR during observation times of at least $20t_h$, where $t_h = \Gamma^2\tau_T$ is the horizontal thermal diffusion time. In the intermediate regime, $0.53 \lesssim \epsilon \lesssim 0.58$, the behavior was more complicated with large patches of almost ISR growing and competing with large patches of SDC. Sometimes, often after long transients, a patch of ISR grew and filled the entire system. As can be seen in Fig. 3, once a patch of ISR connected two opposing sidewalls it grew via the propagation of two almost flat fronts. The behavior described above is reminiscent of that of an equilibrium finite-size system near a phase transition [4].

We note that the initial pattern evolution showed the brief appearance of spirals for values of the control parameter as low as $\epsilon \approx 0.2$ (as shown in Fig. 2(b)). This observation suggests that the bistability of ISR and SDC may extend to lower control parameter values than those reported here. This conjecture would be in agreement with earlier observations in a larger aspect ratio circular cell ($\Gamma = 78$) in which SDC was found above $\epsilon \approx 0.22$ for similar experimental conditions [8]. It would also be consistent with both experiments [8,11,12,17] and simulations [18] in which it was found that the onset of SDC decreased with increasing system size.

To quantify the transition from SDC to ISR, we cal-

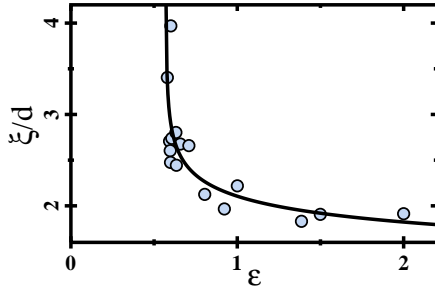


FIG. 4. Correlation length ξ in the spatiotemporal chaotic regime.

culated several statistics in the vicinity of the transition. On the SDC side of the transition, we measured the correlation length ξ from the exponential decay of the autocorrelation function:

$$C(\Delta\vec{x}) = \langle (u(\vec{x} + \Delta\vec{x}, t) - \langle u \rangle) (u(\vec{x}, t) - \langle u \rangle) \rangle_{\vec{x}, t}, \quad (1)$$

where $u(\vec{x}, t)$ is the intensity of the shadowgraph picture. The autocorrelation function is obtained from the Fourier transform of the power spectrum averaged over the duration of each experimental run [19]. As shown in Fig. 4, the correlation length appears to diverge at a *finite* ϵ . The solid line in Fig. 4 is given by $\xi = 1.9d(\epsilon - 0.57)^{-0.12}$. This result is surprising since in an experiment with circular geometry the correlation length was found to diverge as $\xi \propto \epsilon^{-0.43}$ [8,12]. It should be noted, however, that in the same circular experiment [12] the measured data for the correlation time was consistent with a divergence at finite ϵ , with an apparent transition between two chaotic states. In our experiment, however, we observed a transition between a spatiotemporal chaotic state and a stationary state. These apparent discrepancies may be explained by the incompatibility of the circular geometry with ISR, as discussed above.

To further quantify the transition between SDC and ISR, we have calculated the spectral pattern entropy [20,21]. This quantity is defined through a spectral distribution function:

$$p(\vec{k}, t) = \frac{|\Psi(\vec{k}, t)|^2}{\int d^2k |\Psi(\vec{k}, t)|^2}, \quad (2)$$

where $\Psi(\vec{k}, t)$ is the Fourier transform of the two dimensional pattern at time t . Using this distribution function, the spectral pattern entropy $S(t)$ can be defined as:

$$S(t) = - \int d^2k p(\vec{k}, t) \ln p(\vec{k}, t). \quad (3)$$

$S(t)$ measures the disorder in the pattern. For example, if the pattern is ideal (only one mode is excited) $S = 0$ and otherwise $S > 0$.

In Fig. 5 the time evolution of the pattern entropy is shown for $\epsilon = 0.554$. The patterns at the marked places

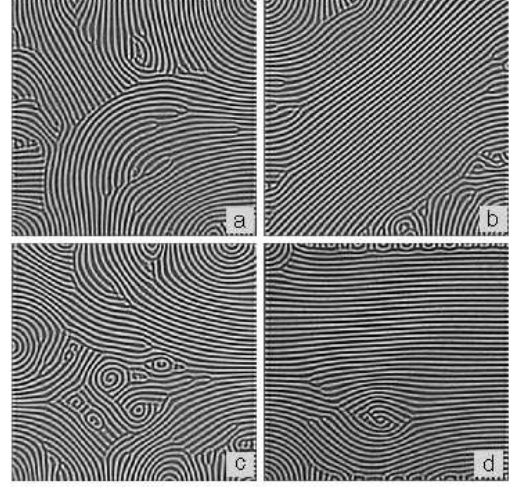
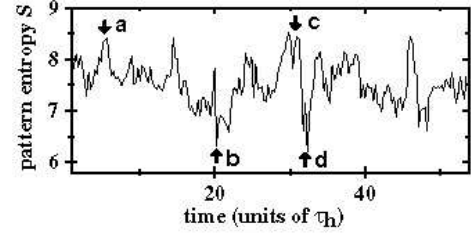


FIG. 5. Time evolution of the pattern entropy $S(t)$ and the pattern for $\epsilon = 0.554$ at times (a) $14.52\tau_h$, (b) $20.27\tau_h$, (c) $30.95\tau_h$, and (d) $32.32\tau_h$.

show a clear correlation with the value of the pattern entropy. As can be seen in Figs. 5(a) and 5(c), patterns with disordered or curved regions lead to large values of $S(t)$, while patterns with straight regions, such as those in Figs. 5(b) and 5(d), lead to small values of $S(t)$. The latter two patterns also show that during the evolution, well-ordered regions were typically aligned either diagonally or perpendicularly to one of the sidewalls of the cell; it appeared that the pattern was probing the system's symmetries.

The experimental data are summarized in Fig. 6 [22]. Fig. 6(a) shows the temporal average of the pattern entropy $\langle S \rangle_t$ as a function of ϵ . As the transition to ISR is approached from above, $\langle S \rangle_t$ shows a sharp decrease. Fig. 6(b) shows the variance $\sigma(S)$ over the same range of ϵ . As the transition is approached, $\sigma(S)$ displays a sharp increase. The location of the sharp changes is consistent with the divergence of the correlation length in Fig. 4. For larger ϵ the variance $\sigma(S)$ approaches a small value, suggesting that the system consists of many independent, fluctuating subsystems. Again, the behavior shown in Fig. 6 appears to be similar to that of equilibrium phase transitions [4].

For a fluid of Prandtl number $\sigma = 1.1$ in a square convection cell of large aspect ratio, we have found a competition between spiral defect chaos and ideal straight roll

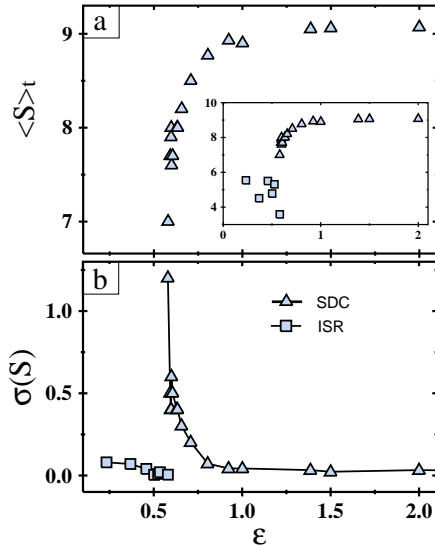


FIG. 6. (a) The time-averaged pattern entropy $\langle S \rangle_t$ and (b) variance $\sigma(S)$ as a function of ϵ . The inset in (a) shows data for both SDC and ISR.

states. This competition is particularly evident in the interplay of disordered regions and straight roll regions during the evolution of the SDC states. Using spatial correlation lengths and statistics based on the spectral pattern entropy, we have provided quantitative evidence for a transition between SDC and ISR at a finite value of ϵ . This transition shows many similarities to transitions in finite-size equilibrium systems, including an intriguing intermittent behavior near the transition. We are currently investigating whether experiments in cells of different aspect ratios can be used to predict the onset of SDC in infinitely extended systems.

We thank W. Pesch and J. Sethna for many fruitful discussions. We are grateful to R. Ragnarsson who provided essential programming for the operation of the experiment. This work was supported by the National Science Foundation through Grants DMR-9320124 and ASC-9503963. E.B. acknowledges support from the Alfred P. Sloan Foundation, D.A.E. from the Cornell Theory Center, and B.B.P. from the Department of Education.

* Presently at the Department of Applied Physics, Columbia University

† Also the Cornell Theory Center, Cornell University, Ithaca, NY 14853.

‡ E-mail: eb22@cornell.edu.

- [1] M. C. Cross and P. C. Hohenberg, Rev. Mod. Phys. **65**, 851 (1993) and references therein.
- [2] J. P. Gollub, Nature **367**, 318 (1994).

- [3] M. C. Cross and P. C. Hohenberg, Science **263**, 1569 (1994).
- [4] See, for example, J. J. Binney, N. J. Dowick, A. J. Fisher, and M. E. J. Newman, *The Theory of Critical Phenomena* (Clarendon Press, Oxford, 1993).
- [5] L. D. Landau and E. M. Lifshitz, *Fluid Mechanics* (Pergamon Press, Oxford, 1959).
- [6] R. M. Clever and F. H. Busse, J. Fluid Mech. **65**, 625 (1974).
- [7] V. Croquette, Contemporary Physics **30**, 113 (1989).
- [8] S. W. Morris, E. Bodenschatz, D. S. Cannell, and G. Ahlers, Phys. Rev. Lett. **71**, 2026 (1993).
- [9] R. V. Cakmur, B. B. Plapp, E. Bodenschatz, and W. Pesch (in preparation). The experimental cell and the material parameters were identical to the ones in this Letter.
- [10] J. R. deBruyn *et al.*, Rev. Sci. Instrum. **67**, 2043 (1996) and references therein.
- [11] J. Liu and G. Ahlers, Phys. Rev. Lett. **77**, 3126 (1996).
- [12] S. W. Morris, E. Bodenschatz, D. S. Cannell, and G. Ahlers, Physica D **97**, 164 (1996) and references therein.
- [13] J. P. Gollub and J. F. Steinman, Phys. Rev. Lett. **47**, 505 (1981); J. P. Gollub, A. R. McCarriar, and J. F. Steinman, J. Fluid. Mech. **125**, 259 (1982).
- [14] Since the top plate temperature was fixed and the bottom temperature was varied, the mean temperature and thus the fluid parameters changed for each ϵ . For each mean temperature a material parameter program [10] was used to calculate the critical temperature difference and the other parameters. We found $\sigma = 1.103 - 0.016\epsilon$, $\tau_T = 2.630 - 0.071\epsilon$, and the non-Boussinesq parameter $\mathcal{P} = -0.481 + 0.024\epsilon$.
- [15] E. Bodenschatz, J. R. deBruyn, G. Ahlers and D. S. Cannell, Phys. Rev. Lett. **67**, 3078 (1991).
- [16] At two opposing sides of the square, the paper was cut in such a way that the top four sheets were recessed by 1 mm, while the other sides were not modified. We found no experimental evidence that the unequal boundaries caused the ISR state to be preferentially aligned. In the figures the stepped boundaries are at the left and right and the non-stepped are at the top and bottom.
- [17] Y. Hu, R. E. Ecke, and G. Ahlers, Phys. Rev. Lett. **74**, 391 (1995); Phys. Rev. E **51**, 3263 (1995).
- [18] W. Decker, W. Pesch, and A. Weber, Phys. Rev. Lett. **73**, 648 (1994).
- [19] In the vicinity of the transition from SDC to ISR, the autocorrelation function was spatially anisotropic. We report lengths computed in the direction in which the correlations decayed slowest.
- [20] M. Neufeld and R. Friedrich, Int. J. Bifurcation and Chaos **4**, 1155 (1994).
- [21] H. W. Xi and J. D. Gunton, Phys. Rev. E **52**, 4963 (1995).
- [22] In Fig. 6, the points labeled as SDC only include those experimental runs for which SDC appeared to be the asymptotic state. It is interesting to note that in the intermittent regime, $0.53 \lesssim \epsilon \lesssim 0.58$, statistics measured during the *disordered* portion of the transient are consistent with the plotted data.